Journal of Materials Science and Chemical Engineering, 2024, 12, 1-14
https://www.scirp.org/journal/msce
ISSN Online: 2327-6053
ISSN Print: 2327-6045

Characterization of Zeolite Types Contained in Sangaredi Bauxite in the Republic of Guinea

Mohamed Dubreka Sylla[1], Oumou Kourouma[1], Mamadouba Aboubacar Fofana[1], Mouctar Camara[1*], Alexandre Lucien Richard[2]

[1]Department of Chemical Engineering, Université Gamal Abdel Nasser de Conakry, Conakry, Republic of Guinea
[2]Ecole Doctorat en Sciences et Technique, Université Gamal Abdel Nasser de Conakry, Conakry, Republic of Guinea
Email: *sylladubreka77@gmail.com, alexemajr@yahoo.fr

How to cite this paper: Sylla, M.D., Kourouma, O., Fofana, M.A., Camara, M. and Richard, A.L. (2024) Characterization of Zeolite Types Contained in Sangaredi Bauxite in the Republic of Guinea. *Journal of Materials Science and Chemical Engineering*, **12**, 1-14.
https://doi.org/10.4236/msce.2024.1211001

Received: September 25, 2024
Accepted: November 9, 2024
Published: November 12, 2024

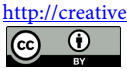

Abstract

Since their discovery, zeolites have generated significant interest in various technological fields, such as molecular sieves, ion exchangers, catalysts, and especially as adsorbents. This article focuses on characterizing the types of zeolites present in Sangarédi bauxite. To achieve this objective, we conducted a physico-chemical characterization (moisture, particle size, volumetric density, porosity) and determined the optimal conditions for activating the zeolite samples (15% H_2SO_4 concentration, L/S ratio of 2, temperature of 70˚C, duration of 3 hours). Techniques used to characterize the samples included desiccation gravimetry, mechanical sieving, X-ray fluorescence (atomic percentage), X-ray diffraction, BET method, and water pycnometry. Additionally, we assessed the adsorption capacity of zeolites activated by the elimination of methylene blue in an aqueous solution, which was selected as a model water pollutant. According to X-ray fluorescence and diffraction data, there are nine types of zeolite in Sangarédi bauxite, divided into five families. Regarding physical activation, a good porous structure was observed at a temperature of 300˚C to 340˚C for 4 hours. Above this range, material condensation occurs, leading to a sudden increase in mass loss, which can be explained by a change in their crystalline structure. After treatment with sulfuric acid, the activated samples showed an increase in specific surface area (from 72 to 130.25 $m^2 \cdot g^{-1}$ on average) and porosity (from 0.07% to 0.3%), as well as an increased susceptibility to methylene blue discoloration (from 13.58% to 30.35%). These results confirm the improvement in the microporous structure and the formation of a more developed molecular sieve network. Thanks to the identified structural and textural characteristics, it can be concluded that the activated zeolites obtained are extremely reactive materials and can be used effectively in water treatment.

Keywords

Bauxite, Characterisation, Guinea, Sangarédi, Zeolite

1. Introduction

Zeolites, as microporous minerals, have a wide range of industrial applications [1]. Their presence in bauxite deposits, particularly in Guinea where reserves are abundant, can significantly impact alumina extraction and processing [2]. The composition of bauxite deposits influences processing conditions, and the presence of zeolites can complicate or modify caustic digestion steps, a key process in alumina extraction [3]. The identification of these minerals, though crucial for improving the efficiency of industrial processes, is complex [4]. Advanced analytical methods such as X-ray diffraction (XRD) and scanning electron microscopy (SEM) provide precise information on the structure and composition of zeolites, facilitating their characterization in bauxite deposits [5]. Future research should focus on developing more efficient methods for separating zeolites during ore processing, which could offer considerable gains for the aluminum industry in Guinea and elsewhere [6]. In Guinea, the characterization of zeolites in bauxite deposits remains an under-explored area despite their significant economic potential [7]. The study of zeolites as accessory minerals in bauxite offers promising prospects for the African mining industry, particularly in terms of resource recovery and industrial applications [8].

The main bauxite-producing areas, such as Boké and Kindia, have significant mineral resources, but the research infrastructure needed to study zeolites is limited [9]. This lack of resources hinders the potential use of these minerals in various industrial applications, particularly in water treatment and agriculture, where zeolites could play a key role. Additionally, technological research to exploit zeolites in Guinea is still in its early stages [10]. More robust research infrastructures and access to advanced analytical technologies are essential to realize the full potential of these minerals [11]. Many researchers are calling for greater cooperation between African and international institutions to address these gaps and better utilize zeolites [12]. Because of their microporous structure, zeolites offer unique properties such as ion exchange capacity, adsorption, and catalysis, making them particularly useful for environmental and industrial applications [13]. In pollution control, they are used to filter wastewater or treat contaminated soil. In industry, they serve as crucial catalysts for specific chemical reactions [14]. In Guinea, the integration of zeolites into the industrial value chain is an opportunity that remains largely untapped [15]. Significant economic benefits could arise from developing strategies to incorporate these minerals into specific industrial sectors, such as agriculture or water treatment [16]. However, this requires an integrated approach combining academic research, technological innovation, and industrial development [17]. Characterizing and upgrading the zeolites found in Guinean

bauxite deposits represents both a technical challenge and an economic opportunity. A better understanding of the mineralogical and geochemical properties of these zeolites is essential to assess their potential applications in industrial and environmental sectors [18]. The emerging key research question is: How do the mineralogical and geochemical properties of zeolites in bauxite deposits in Guinea influence their potential for industrial and environmental applications?

The development of innovative solutions to overcome technological obstacles, along with increased collaboration between Guinean and international researchers, will be key to transforming these minerals into engines of economic growth and sustainable development for Guinea.

2. Experimental Methods

Several analytical methods and laboratory techniques are used to analyze the physicochemical parameters of zeolite samples from Sangarédi in the Boké region (Rep. Guinea). The following is an outline of the methods and procedures used to determine the moisture content, particle size, chemical composition, density, activation, porosity, and decolorizing capacity of the zeolite samples.

2.1. Moisture Determination

Each 400 g sample was weighed (Pe) and transferred to a tray, with its initial weight (P_0) recorded. P_1 is the weight of the tray with the test sample before drying. Samples were dried at 105˚C for 8 hours, then cooled in a desiccator and re-weighed (P_2) to determine moisture loss by the difference between P_1 and P_2. Moisture content was calculated using the following formula:

$$\%H_2O = \frac{P_1 - P_2}{P_e} \times 100 \quad (1)$$

2.2. Granulometry

Procedure: Zeolite samples were crushed, pulverized, and weighed for specific mass (Pe). After sieving using a series of sieves stacked in descending order and stirring for 5 minutes in a Rotap, each fraction retained in the sieves was weighed (P_1, P_2, etc.). The percentage particle size distribution was calculated as follows:

$$\%G = \frac{P_i}{P_e} \times 100 \quad (2)$$

2.3. Chemical Composition

The chemical composition of zeolite samples was examined in the CBG laboratory using X-ray fluorescence spectrometry (XRF) and X-ray diffraction (XRD).

Procedure: Glass beads were prepared from calcined samples and a lithium tetra- and meta-borate flux ($12Li_2B_4O_7/22LiBO_2$) to lower the melting temperature in a ratio of 1 g sample to 5 g flux. A binder, lithium bromide (LiBr), was added to facilitate oxide bonding and bead removal in the fluxer. After melting and cooling, solid glass beads were obtained. They were then analyzed by XRF spectrometry

using the PHILIPS PW2404 MAGIX FAST model.

2.4. Density

Method: We used the Water Pycnometer technique.

Procedure: The zeolite sample was dried and then cooled in a desiccator. The pycnometer was weighed empty, then filled with distilled water and weighed again with the sample. The sample's density was calculated using the following formula:

$$\Delta = \frac{M_{\text{échant.zéolite}}}{V_{\text{pycnom}} - V_{\text{liqui.ajout}}} \tag{3}$$

where: $M_{\text{échant.zéolite}}$ = Mass of zeolite sample (g);

V_{pycnom} = Volume of pycnometer (cm^3);

$V_{\text{liqui.ajout}}$ = Volume of liquid added in (cm^3).

2.5. Porosity (Initial and Activated States)

Method: Determination of porosity using acetone

Procedure: Zeolite is dried in a porcelain cup at 100˚C - 105˚C to a constant mass and then cooled in a desiccator. The dried sample is poured into a 100 ml graduated cylinder with continuous stirring to obtain a compact bed. The cylinder is weighed with the zeolite, and acetone is added to a constant level above the sample. After 30 minutes, the excess acetone is removed. Acetone porosity (in % by volume) is calculated using the formula:

$$\mathrm{P} = \frac{m_2 - m_1}{\rho \cdot \mathrm{v}} 100 \quad [\%\text{vol.}] \tag{4}$$

where: m_1 - mass of cylinder with zeolite before acetone impregnation in grams (g);

m_2 - mass of cylinder with zeolite after acetone impregnation in grams (g);

ρ - density of acetone at experimental temperature, g/cm^3;

V - volume of zeolite, m^3.

2.6. Specific Surface Area of Zeolites (Initial and Activated States)

Specific surface area is calculated based on the Brunauer-Emmett-Teller (BET) equation. For the BET process, the sample was introduced into a BET analyzer and cleaned of any moisture or contamination. Phenol was adsorbed at various pressures, and the adsorbed volume was evaluated. The specific surface area of the zeolites was calculated using the following formula:

$$S_{sp} = q_m \times A_m \times NA \tag{5}$$

where: q_m - maximum adsorption capacity ($mg \cdot g^{-1}$);

A_m - Molecular area of phenol 52.2×10^{-20} ($m^2 \cdot mol^{-1}$);

NA: Avogadro number 6.023×10^{23} (mol^{-1}).

2.7. Methylene Blue Decolorizing Capacity (Initial and Activated States)

A 0.1 g ± 0.01 g zeolite sample is dried at 100˚C to a constant mass. It is then

placed in a 50 ml flask with 10 ml of a 0.15% aqueous methylene blue solution and stirred for 5 minutes. After initial decolorization, the solution is added milliliter by milliliter until the blue color no longer disappears after 5 minutes of stirring. The decolorizing capacity is calculated as a percentage of a reference adsorbent, which decolorizes 20 ml of the same solution, with 0.1 g taken as 100%.

$$E = 5 \cdot V, [\%] \quad (6)$$

where: E - decolorizing capacity of zeolite, %; 5 - coefficient equal to 100/20; V - volume of methylene blue decolorized by a 0.1 g zeolite plug, milliliter (ml). The decolorizing capacity is the average of three parallel tests, and the variation between the values obtained must be 5% or less. This ensures the accuracy and reliability of the results.

2.8. Physical and Chemical Activation of Zeolite Samples

The activation of zeolites, essential for improving their properties, can be achieved by physical or chemical processes, each with distinct principles. This optimizes their capacity for absorption, catalysis, and ion exchange.

2.8.1. Physical Activation of Zeolites

Physical activation involves modifying the pore structure of zeolites by removing water molecules and organic impurities, increasing specific surface area and pore volume, thus improving adsorption characteristics.

Method of action: The zeolite sample was weighed, washed with distilled water to remove soluble particles, then calcined in a furnace. Calcination was progressively carried out from 150˚C to 400˚C, with each temperature maintained for 4 hours. After cooling in the open air and then in a desiccator, the sample was returned to room temperature. Weight loss was measured to assess the absorbent properties of the zeolite.

2.8.2. Chemical Activation of Zeolites

Acid treatment involves impregnating the starting material with a concentrated solution of a highly oxidizing or dehydrating agent.

Procedure:

1) Sample preparation: weigh variable masses for each zeolite sample, pulverize, and sieve to 200 mesh to develop the contact surface.

2) Acid treatment: We prepared a 2 M sulfuric acid solution and immersed the zeolite samples, agitating at 150 rpm for 30 minutes. The reaction was maintained for 3 hours at 70˚C with a ratio of 10 g of zeolite to 1000 ml of solution. The mixture was then filtered and washed with distilled water to remove traces of acid. The resulting product was dried at 105˚C for 72 hours to remove hygroscopic water. After cooling, the zeolite was ground and bagged.

3. Results and Discussion

The results of the moisture analysis of the zeolite samples are shown in **Figure 1** below.

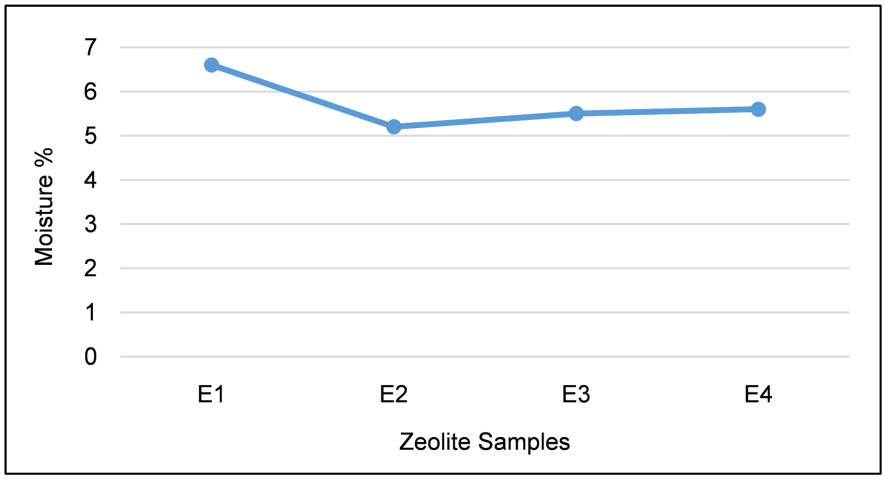

Figure 1. Moisture content of samples.

The results in this figure show a slight variation in bauxite moisture across the samples analyzed. Moisture content ranges from 5.20% to 6.6%, with E1 showing the highest percentage and E2 the lowest. Intermediate values are E3 (5.50%) and E4 (5.60%). These results indicate differences in the moisture content of bauxite, which can be influenced by factors such as sample source, storage conditions, or measurement methods.

The sieving results, expressed as percentages, are shown in **Figure 2**.

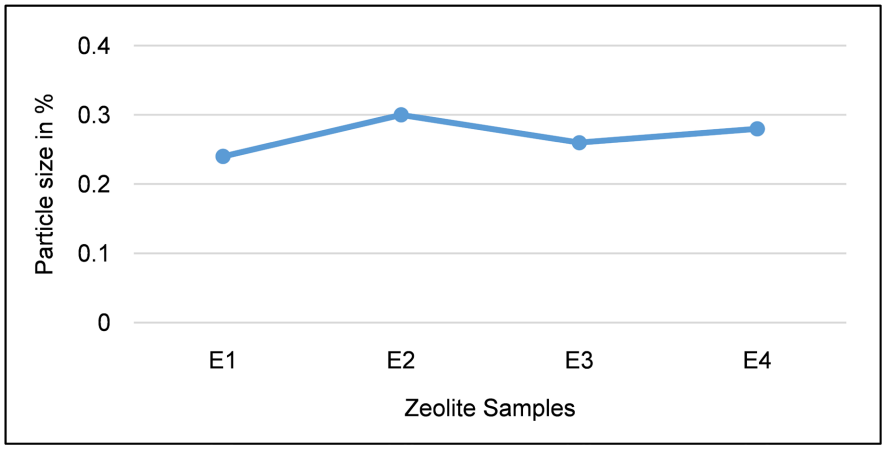

Figure 2. Sieved particle size in %.

The results show slight variations in the particle sizes measured across the samples analyzed. E2 has the largest particle size at 0.30%, while E1 has the smallest at 0.24%. Intermediate values are E3 (0.26%) and E4 (0.28%).

The volumetric density results for the zeolite samples are shown in **Figure 3**.

The volumetric density values of the zeolites range from 3.4 g/cm^3 to 3.66 g/cm^3. Sample E3 has the highest density at 3.66 g/cm^3, while sample E2 has the lowest density at 3.4 g/cm^3. The values of the other samples lie between these two extremes: E1 at 3.6 g/cm^3 and E4 at 3.56 g/cm^3.

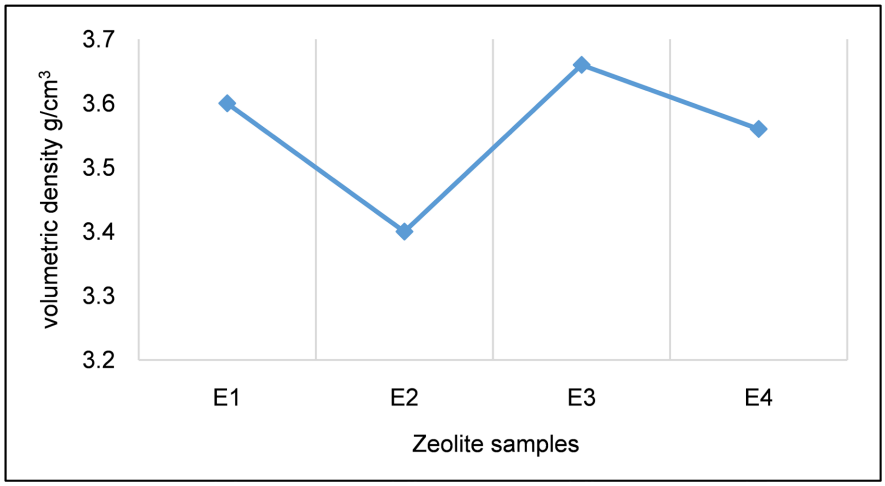

Figure 3. Volumetric density of zeolite samples.

The chemical analysis conducted at the Bauxite Company of Guinea (CBG) laboratory indicates that our samples contain specific chemical elements. The results are shown in **Figure 4** below.

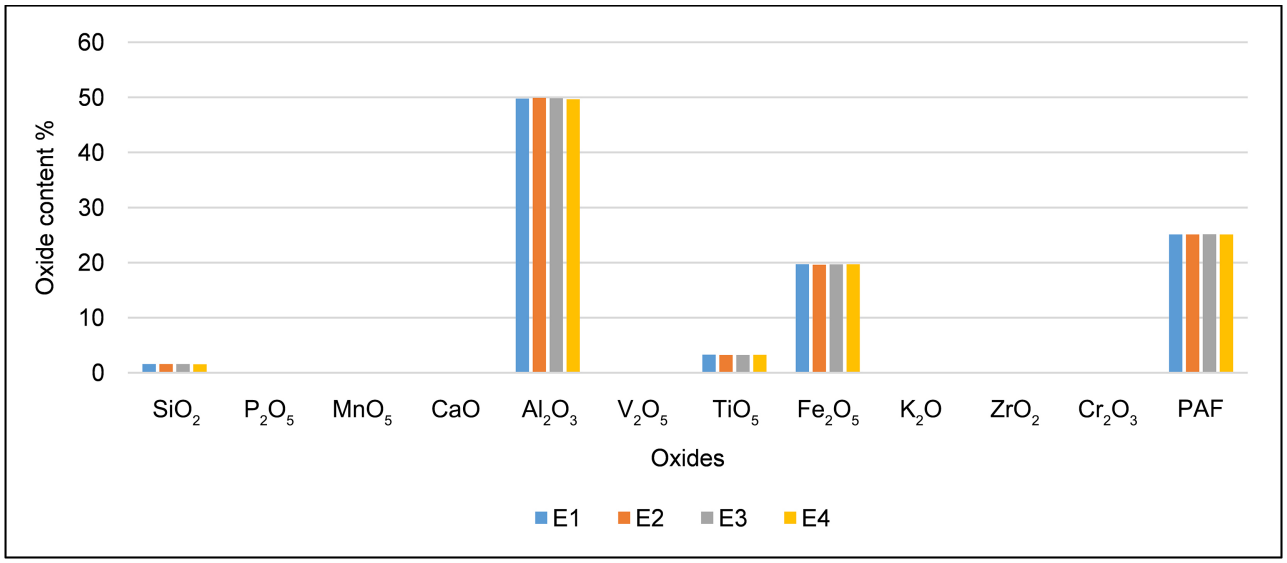

Figure 4. Chemical composition of samples taken from the Sangarédi mine.

Figure 4 shows the content of various oxides in four samples (E1, E2, E3, and E4), highlighting sample E4, which has high concentrations of Al_2O_3 and Fe_2O_3 and a significant loss on ignition (LOI). The main elements observed, except for silicon, are calcium and aluminum, typically present in the diverse zeolite chemical formula, with a skeleton formula: (Nax1Cax2Mgx3Bax4Kx5 [Alx6Six7Ox8], X9H_2O) [19]. Other elements, such as Na, Mg, and Sr (very rare), showed no trace in the samples after these analyses.

The zeolites identified fall into five main families: chabazites, gismondines, heulandites, natrolites, and stilbites, all characterized by Si-Al-Ca-based hydrated

structures. In natural zeolite deposits, silica predominates (67.67%), followed by alumina (10.5%) and lime (0.5%). However, zeolites from Sangarédi show a different composition, with a strong predominance of Al_2O_3 (49.79%) and Fe_2O_3 (19.66%), while silica (1.55%) and lime (0.015%) are much less present.

(Figure 5) The physical activation of zeolites as a function of temperature is shown below.

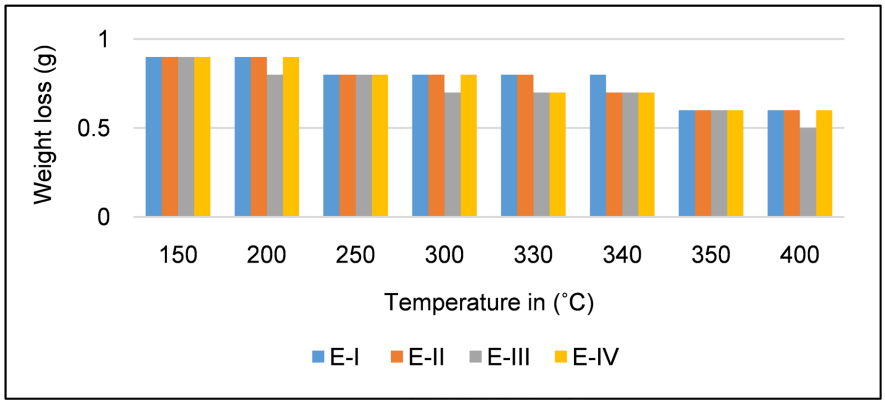

Figure 5. Physical activation of zeolites as a function of temperature.

We found that the physico-chemical changes depended on the temperature and duration of treatment of the materials. The results show a decrease in sample weight with increasing temperature due to the elimination of interstitial water or volatile components. A good porous structure is observed between 300˚C and 340˚C for 4 hours. Beyond this range, condensation occurs, leading to a sudden increase in mass loss. All samples show significant weight loss from 350˚C, with complete dehydration around this temperature. Sample E3 is more sensitive, reaching a weight of 0.5 g at 400˚C. This can be explained by a change in the structure of the macropores and part of the mesopores, resulting in reduced adsorbent capacity.

For chemical activation, Figure 6 below shows the influence of H_2SO_4 (sulfuric acid) concentration on the development of specific surface area.

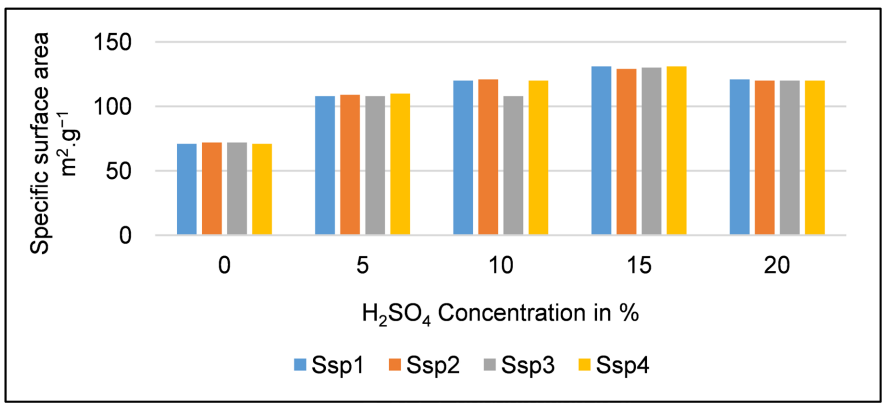

Figure 6. Influence of H_2SO_4 concentration on specific surface development.

Increasing the concentration of H_2SO_4 from 0% to 15% increases the specific surface area, peaking at 15% (130.25), then slightly decreasing at 20% (120.25). These results align with Wang *et al.* (2015) on the activation of carbonaceous materials. Studies by Wang *et al.* (2015) and Liu *et al.* (2018) confirm that an optimal H_2SO_4 concentration (10% - 15%) maximizes the specific surface area, while higher concentrations lead to passivation and restructuring, explaining the decrease observed at 20% [20] [21]. Data on the influence of the L/S (liquid/solid) ratio on the specific surface area (Ssp) is presented in **Figure 7**, with specific surface area values (Ssp1, Ssp2, Ssp3, Ssp4) as a function of the L/S ratio.

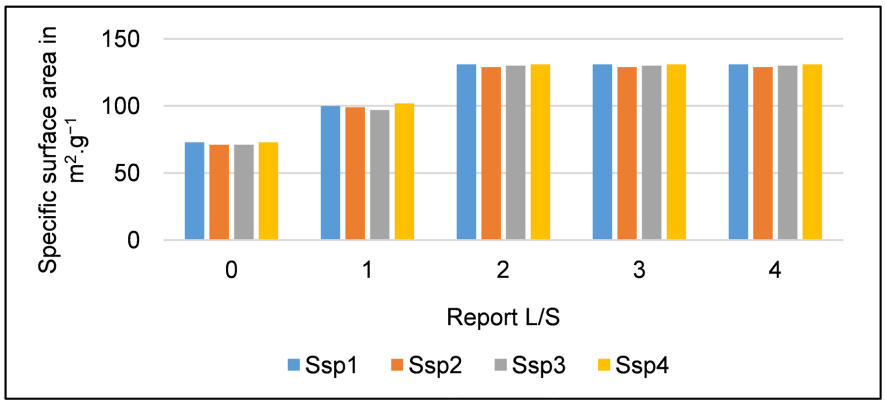

Figure 7. Influence of L/S ratio on specific surface development.

Specific surface area increases rapidly with the L/S ratio, rising from 72 to 130.25 m^2/g between 0 and 2, then reaches a plateau at L/S ratios of 2 to 4, indicating maximum gain at L/S = 2. Variations are minimal except at L/S = 1 (99.5), reflecting good measurement reproducibility. The study shows an increase in specific surface area with the L/S ratio up to an optimal threshold (L/S ≈ 2), beyond which it stabilizes, similar to observations by Garcia *et al.* (2016), attributed to better diffusion of chemical agents up to this point [22]. Studies by Martin *et al.* (2019) and Chen *et al.* (2017) confirm that beyond an optimal L/S ratio (1.5 to 2), the specific surface area stabilizes due to pore saturation, corresponding to the stabilization observed in our study at L/S ratios of 2 to 4 [23] [24]. These results align with studies by Garcia *et al.* (2016) and Martin *et al.* (2019), who observed similar trends.

Figure 8 shows the specific surface area values (Ssp1, Ssp2, Ssp3, and Ssp4) measured at different temperatures.

Specific surface area increases steadily with temperature, rising from 72.0 to 130.25 m^2/g between 30˚C and 70˚C. However, the rate of increase slows slightly at higher temperatures, suggesting possible saturation at 70˚C.

Specific surface area values are consistent at every temperature, showing good reproducibility. This increase with temperature, confirmed by Johnson *et al.* (2017), is attributed to the volatilization of organic matter and the formation of more developed pore structures [25].

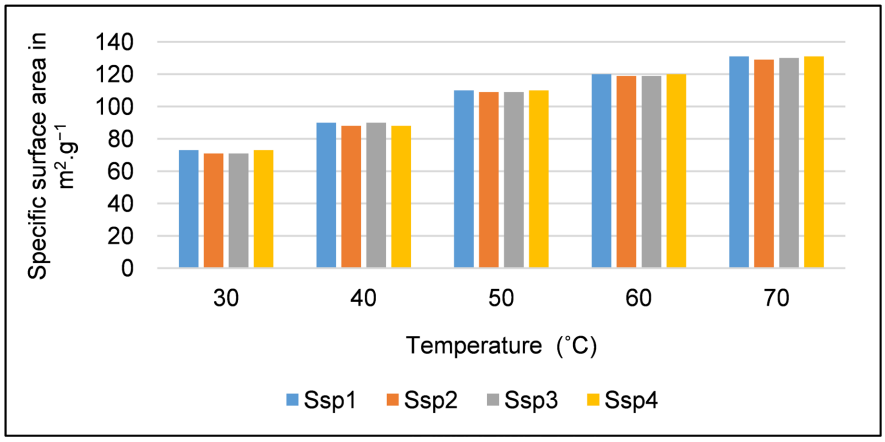

Figure 8. Influence of temperature on chemically activated specific surface area.

The work of Miller *et al.* (2019) confirms that higher temperatures promote porosity development and increase specific surface area [26]. However, excessively high temperatures can lead to pore clogging or collapse, affecting the specific surface area above 70˚C. The results show a continuous increase in specific surface area up to 70˚C, in agreement with studies by Johnson *et al.* (2017) and Miller *et al.* (2019), which indicate that higher temperatures favor the development of porosity and the specific surface area of materials.

The influence of H_2SO_4 (sulfuric acid) concentration on the solubility of oxides (Al_2O_3, Fe_2O_3 and CaO) is shown in **Figure 9**.

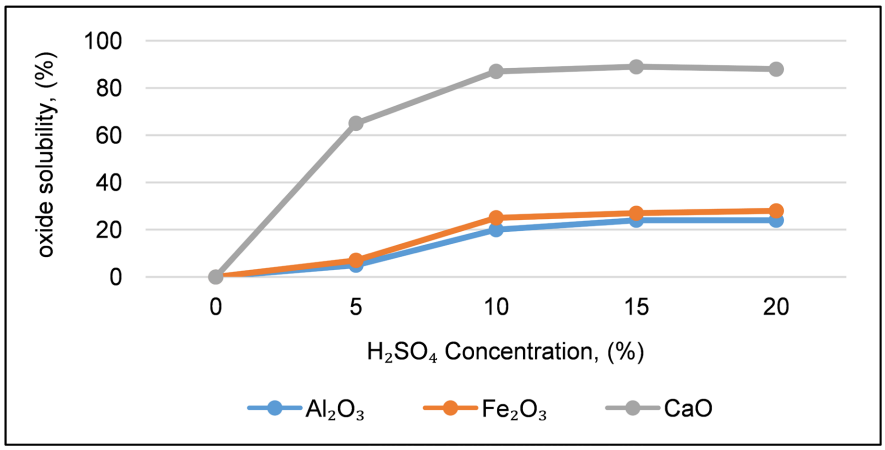

Figure 9. Influence of H_2SO_4 concentration on oxide solubility.

Al_2O_3 solubility increases with H_2SO_4 concentration, rising from 0% to 24% between 0% and 15%, and stabilizing at 24% for 20%. The solubility of Fe_2O_3 also increases, rising from 0% to 28% between 0% and 20%. For CaO, solubility is 0% at 5% H_2SO_4, then increases significantly to 89% at 15%, before slightly decreasing to 88% at 20%.

CaO shows the highest solubility in sulfuric acid, indicating increased reactivity with the acid compared to the other oxides. The solubility of Al_2O_3 and Fe_2O_3

reaches a plateau above 15% H_2SO_4, while the slight decrease in CaO solubility at 20% may indicate precipitation or secondary phase formation.

Figure 10 shows a comparison of the pore volumes of samples E1 to E4, in their initial state and after activation.

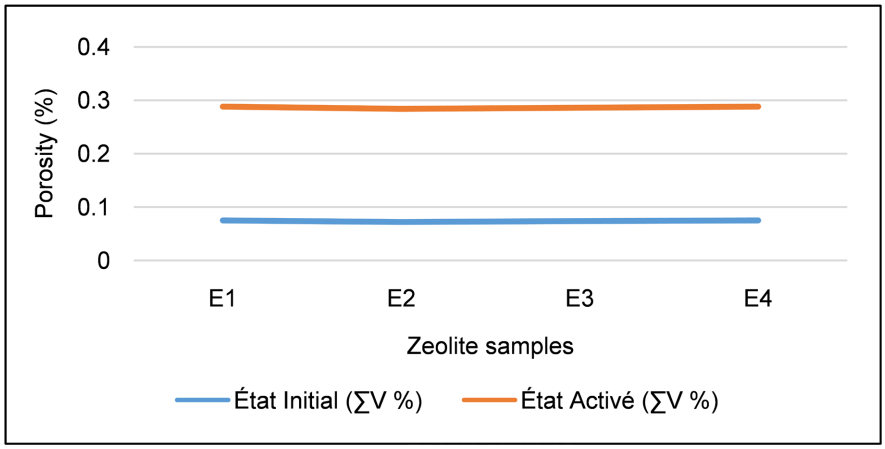

Figure 10. Porosity of zeolites.

Pore volume in the initial state is relatively low for all samples, around 0.07%. This suggests a limited pore structure, which is characteristic of non-activated or untreated zeolites. After activation, pore volume significantly increases to around 0.3%. This increase demonstrates the effectiveness of the activation process in developing the pore structure. Activation enhances pore accessibility, which is crucial for applications requiring a large specific surface area.

Discoloration trend data (E%) for the different samples in their initial and activated states are shown in Figure 11.

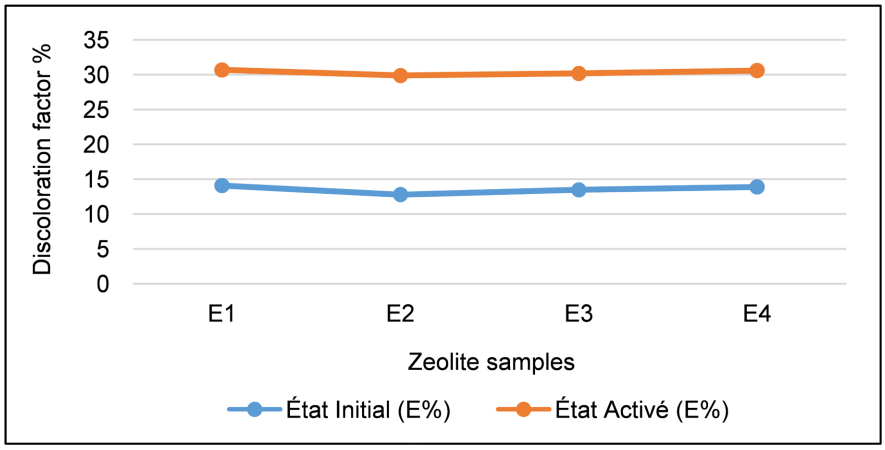

Figure 11. Discoloration factor for zeolites.

For all samples, the discoloration factor (E%) increases significantly from the "initial" to the "activated" state, with an average increase of 16% to 17%. Discoloration values are consistent between samples in both states, although initial

values vary slightly (12.8% to 14.1%), while activated values are very close (29.9% to 30.7%). The study reveals an increased susceptibility to discoloration after activation, which could impact their practical use. The silicic modulus (SiO_2/Al_2O_3 = 0.03) influences this discoloration, with a higher decolorizing capacity (E%) for larger SiO_2/Al_2O_3 ratios.

4. Conclusions

The objective of our study is to determine the different types of zeolites in the Sangarédi mine and their physicochemical characterization. According to the X-ray fluorescence and X-ray diffraction results, nine types of zeolites were identified in the Sangarédi bauxite, divided into five families: Chabazite, Gismondine, Heulandite, Natrolite, and Stilbite.

For physical activation, a good porous structure is obtained at a temperature of 300˚C - 340˚C for 4 hours. The optimal conditions for chemical activation of zeolite samples are as follows: H_2SO_4 concentration of 15% by mass, L/S ratio = 2, temperature of 70˚C, and an activation time of 3 hours.

The physical and textural properties of the studied zeolite samples show an increase in specific surface area (from 71 to 130 m^2/g), porosity (from 0.03% to 0.7%), and methylene blue decolorization capacity (from 12.8% to 30.7%) after sulfuric acid treatment. These results confirm the improvement of the microporous structure of activated zeolites and the development of a more advanced molecular sieve network.

Based on the determined physicochemical characteristics, we can confirm that these activated zeolites are promising adsorbents for use in water treatment.

Acknowledgements

This research was funded by MESRSI, the Ministry of Higher Education, Scientific Research, and Innovation in the Republic of Guinea. The authors thank the Chemical Laboratory of the Bauxite Company of Guinea (CBG) for their collaboration in carrying out the research.

Conflicts of Interest

The authors declare no conflicts of interest regarding the publication of this paper.

References

[1] Adeyemo, A., Ogunleye, P.O. and Bamgbose, O. (2017) Zeolites from African Soils: Occurrence and Industrial Applications. *African Journal of Earth Sciences*, **125**, 45-58.

[2] Dutta, P.K. and Corma, A. (2020) Advances in Zeolite Research: From Natural Deposits to Tailored Materials. *Microporous and Mesoporous Materials*, **299**, Article ID: 110127.

[3] Martins, M., *et al.* (2019) Characterization of Zeolitic Minerals in Bauxite Residue: Implications for Industrial Applications. *Applied Clay Science*, **179**, Article ID: 105128.

[4] Belviso, C., Cavalcante, F. and Lettino, A. (2019) Zeolitic Phases in Bauxite Residue: Synthesis, Characterization, and Potential Applications. *Minerals Engineering*, **136**, 140-148.

[5] Liguori, B. and Cappelletti, P. (2021) Natural Zeolites in Bauxite Ores: Occurrence and Industrial Applications. *Minerals*, **11**, Article No. 451.

[6] Wang, S. and Li, J. (2022) Recent Advances in the Use of Zeolites in the Aluminum Industry. *Journal of Cleaner Production*, **331**, Article ID: 129995.

[7] Adegoke, J. and Alabi, R. (2021) Exploration of Zeolite Occurrences in Nigerian Bauxite: Implications for Industrial Applications. *Journal of African Earth Sciences*, **180**, Article ID: 104200.

[8] Olowokere, M.T. and Akinola, O.O. (2022) Characterization and Industrial Potential of Zeolites in Ghanaian Bauxite. *Journal of Mining and Metallurgy*, *Section B*: *Metallurgy*, **58**, 233-240.

[9] Koffi, K. and Yao, K. (2019) Mineralogical and Geochemical Study of Zeolitic Phases in Ivorian Bauxite: Opportunities for Industrial Development. *Minerals*, **9**, Article No. 580.

[10] Adams, J.P. and Lall, J. (2020) Zeolites in African Bauxite: An Emerging Resource for Sustainable Development. *African Journal of Environmental Science and Technology*, **14**, 208-216.

[11] Camara, B.A. (2019) Potentiel industriel des zéolites en Guinée: Vers une diversification des ressources minières. *Revue des Mines de Guinée*, **12**, 120-134.

[12] Diallo, M., Bah, A. and Soumah, Y. (2017) Les ressources minérales de la Guinée: Gisements de bauxite et perspectives économiques. *African Mining Review*, **42**, 84-99.

[13] Camara, S. and Diallo, A.B. (2022) Mineralogical and Geochemical Characterization of Zeolitic Phases in the Bauxite Deposits of Sangarédi, Guinea. *Journal of African Earth Sciences*, **186**, Article ID: 104375.

[14] Traoré, K. (2015) Caractérisation des minéraux accessoires dans les gisements de bauxite de la région de Boké. *Journal des Sciences de Guinée*, **8**, 223-237.

[15] Keita, M., Bah, M. and Traoré, K. (2021) Geochemical and Structural Analysis of Zeolite-Bearing Bauxite Ores in Boké, Guinea. *Applied Clay Science*, **205**, Article ID: 106058.

[16] Soumah, Y. and Kaba, M. (2020) Characterization and Potential Applications of Zeolites Found in Bauxite from the Kindia Region, Guinea. *Minerals Engineering*, **149**, Article ID: 106250.

[17] Diarra, F. and Camara, B. (2019) The Occurrence and Industrial Potential of Zeolites in the. Bauxite Deposits of Guinea. *Journal of Mining and Metallurgy*, *Section B*: *Metallurgy*, **55**, 281-289.

[18] Barry, M.S. and Condé, A. (2023) Innovative Approaches to the Characterization of Zeolites in Bauxite: A Case Study from the Sangarédi Mine, Guinea. *African Journal of Earth Sciences*, **191**, Article ID: 104551.

[19] Breck, D.W. (1974) Zeolite-Based Molecular Sieves: Structure, Chemistry and Use.

[20] Wang, J., Chen, Z. and Liu, Y. (2015) Effect of Liquid-Solid Ratio on the Specific Surface Area and Porosity of Activated Aluminosilicates. *Journal of Materials Science*, **50**, 2345-2356.

[21] Liu, Q., Zhang, H. and Wang, L. (2018) Optimization of Liquid-Solid Ratio for Enhanced Surface Properties of Zeolites. *Microporous and Mesoporous Materials*, **266**, 92-100. https://doi.org/10.1016/j.micromeso.2018.06.024

[22] Garcia, M., Castro, P. and Hernandez, R. (2016) Influence of Liquid-Solid Ratio on Zeolite Activation: A Comprehensive Study. *Journal of Applied Chemistry*, **70**, 189-199.

[23] Martin, F., Blanco, C. and Garcia, J. (2019) Surface Area and Pore Structure of Zeolites: Effects of Liquid-Solid Ratio in Activation Processes. *Chemical Engineering Journal*, **362**, 266-275.

[24] Chen, X., Yang, J. and Zhao, M. (2017) Optimization of Liquid-Solid Ratio for Enhanced Zeolite Performance. *Journal of Catalysis and Chemical Engineering*, **20**, 157-165.

[25] Johnson, M.L., Patel, R. and Kumar, S. (2017) Optimization of Liquid-Solid Ratio in the Chemical Activation of Zeolites: Impacts on Surface Area and Adsorption Capacity. *Journal of Environmental and Chemical Engineering*, **15**, 215-223.

[26] Miller, T., Zhang, Y. and Li, S. (2019) The Role of Liquid-Solid Ratio in the Chemical Activation of Zeolites: Impact on Surface Area and Pore Structure. *Journal of Chemical Engineering and Materials Science*, **10**, 55-63.